Preprint
UCRL-JC-137269

Potential Biogenic Corrosion of Alloy 22, A Candidate Nuclear Waste Packaging Material, Under Simulated Repository Conditions

J. Horn, S. Martin,A. Rivera, P. Bedrossian and T. Lian

This article was submitted to
National Association of Corrosion Engineers Corrosion 2000
Orlando, FL
March 26-31, 2000

U.S. Department of Energy
Lawrence Livermore National Laboratory

January 12, 2000

POTENTIAL BIOGENIC CORROSION OF ALLOY 22, A CANDIDATE NUCLEAR WASTE PACKAGING MATERIAL, UNDER SIMULATED REPOSITORY CONDITIONS

Joanne Horn, Sue Martin, Angel Rivera, Peter Bedrossian, and Tiangan Lian
Lawrence Livermore National Laboratory
P.O. Box 808, L-204
Livermore, CA 94550

ABSTRACT

The U.S. Department of Energy has been charged with assessing the suitability of a geologic nuclear waste repository at Yucca Mountain (YM), NV. Microorganisms, both those endogenous to the repository site and those introduced as a result of construction and operational activities, may contribute to the corrosion of metal nuclear waste packaging and thereby decrease their useful lifetime as barrier materials. Evaluation of potential Microbiological Influenced Corrosion (MIC) on candidate waste package materials was undertaken in reactor systems incorporating the primary elements of the repository: YM rock (either non-sterile or presterilized), material coupons, and a continual feed of simulated YM groundwater. Periodically, both aqueous reactor efflux and material coupons were analyzed for chemical and surfacial characterization. Alloy 22 coupons exposed for a year at room temperature in reactors containing non-sterile YM rock demonstrated accretion of chromium oxide and silaceous scales, with what appear to be underlying areas of corrosion.

INTRODUCTION

The U.S. Department of Energy is assessing the suitability and design of a potential nuclear waste repository at Yucca Mountain (YM), Nevada. Waste Packages (WP) housed within the repository are projected to contain commercial spent nuclear fuels as well as high-level nuclear defense wastes. The present design of WP includes an outer barrier composed of Alloy 22 (UNS N06022; a Ni-Cr-Mo alloy that is intended to provide corrosion resistance), and an inner barrier of 316L Stainless Steel (316SS, UNS S31603; to provide structural support and radiation shielding). Native and introduced microorganisms in the repository environment may significantly contribute to the corrosion of these WP materials, especially considering the long time period required for adequate waste containment. Microbiological contributions to WP corrosion must therefore be accounted for to accurately predict the time and mode of WP failure. Determination of bacterial contributions to the corrosion of WP materials is being evaluated under conditions representative of those expected in the proposed repository environment. These determinations will then be factored into an overall model of waste package failure to evaluate the degree of containment afforded by waste packages.

Simulation of a saturated, oxic WP environment (intended to mimic re-entry of YM ground water into the repository drifts) was achieved in a continual-flowthrough reactor (or, "microcosm") fed with a simulated groundwater formulation. The apparatus contained sterilized coupons of Alloy 22 or SS316, and crushed YM rock in a non-sterilized condition (i.e., containing the microorganisms from the post-construction repository environment), or pre-sterilized. Periodically, the chemistry of dissolved metal ions in the aqueous reactor efflux were analyzed. Coupons were also withdrawn, and analysis of the surface chemistry and topography were performed. These collective data provide identification of corrosion products, establish their rates of formation, and indicate modes and rates of biologically-mediated attack, which can be modeled to supplement an overall corrosion code. Comparison of results from systems containing non-sterile YM rock with those obtained from systems with sterilized rock will demonstrate microbial contributions and provide biochemical rate constants, corrosion rates, and the species of observed biogenic corrosion products. Here, we present results of these studies with Alloy 22 from non-sterile systems over an exposure period of one year at room temperature.

APPROACH AND EXPERIMENTAL METHODS

Microcosm Reactor Components

The microcosm apparatus (Fig. 1), a continuous flow-through system, consisted of a borosilicate glass vessel (500 mL) fitted with an inlet for introducing simulated YM ground water (below) from a 2 liter reservoir, and an outlet for draining the spent media. The influx and efflux rates were maintained at an equivalent, constant rate (2 mL/hr) with the aid of peristaltic pumps, to maintain a constant volume (250 mL) of ground water in the vessel (total residence time was approximately 5 days). In-line media break tubes were incorporated into the outlet tubing to prevent back-contamination, and in-line filters (0.2 μm) were included on the inlet tubing to assure sterility of introduced simulated ground water. All components of the system were pre-sterilized, and the sterility of those system elements upstream of the microcosm vessel were maintained and monitored by live plating techniques[1]. Reactors were incubated for a total of one year at ambient laboratory temperature (approximately 22°C).

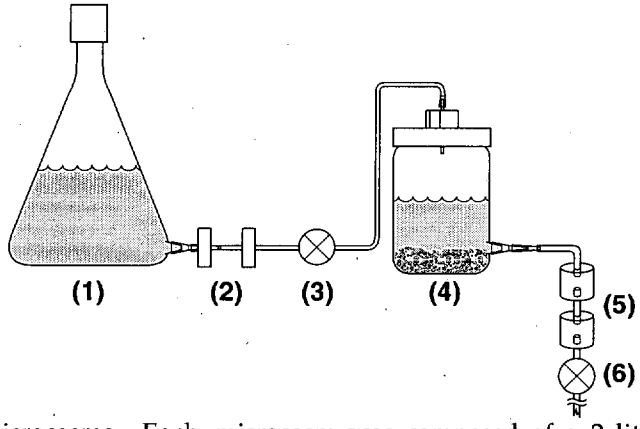

Figure 1. Configuration of microcosms. Each microcosm was composed of a 2 liter reservoir tank containing sterile media (1), that was fed through two 0.2 μm in-line filters (2), by means of a peristaltic pump (3), into a 500 mL modified spin flask that contained crushed YM tuff and test coupon material (4). Media break tubes (5) on the outflow were used to prevent back-contamination, and the outflow rate was regulated by a second peristaltic pump (6).

Simulated ground water (10XJ13 media) was formulated from a ten-fold concentration of YM ground water (well J13 in the YM region[2]) using *The Geochemist's Workbench*[3] (Table 1). To prevent precipitation of minerals due to concentrating the reported ground water composition, and control initial pH, the concentrations of calcium, sodium, and carbonate were decreased (with respect to the reported composition of J13), resulting in near-saturation conditions with respect to mineral phases (Table 1). Available forms of soluble silica (metasilicates) significantly increase the pH of the solution, therefore no silica was added to the simulated 10XJ13 formula. Additionally, the 10XJ13 media was supplemented with 0.1% glucose, a minimal organic carbon source; the final pH was 7.6. Previous studies had shown that this formulation supported microbial growth of organisms contained in YM rock[4].

Table 1. Comparison of calculated 10-fold concentration of natural J13 ground water with simulated J13 water (concentrated 10-fold)

	10X J13[2] ground water	10X J13 simulated water
component	*concentration, mM*	*concentration, mM*
Na	19.100	6.143
K	1.310	1.306
Ca	3.120	2.505e-2
Mg	0.790	0.790
NO_3	1.550	1.553
Cl	1.950	1.951
CO_3	20.500	0.527
SO_4	1.950	1.949
Li	0.061	0
Sr	0.004	0
Al	0.004	0
Fe	0.001	0
Si	9.610	0
F	1.160	1.160
Glucose	0	5.550

In addition to simulated ground water, completed microcosms each contained 20 candidate waste package material coupons [Alloy 22 (Table 2); 3.23 cm^2 surface area per coupon, total coupon surface area was 64.5 cm^2 per microcosm reactor] imbedded vertically in crushed YM rock (100 g); coupons were placed to prevent physical contact between them. Coupons were either placed in reactors containing non-sterilized or pre-sterilized YM rock (below), to permit evaluation of microbiological contributions to observed results. Alloy 22 coupons were prepared by stamping with identification numbers, wet-polished with abrasive paper progressively to 600-grit, and cleaned with distilled water and acetone. Coupons were then weighed for eventual weight-loss analysis before being sterilized (using a ^{60}Co gamma source, 3-4 Mrad total dose), and emplaced in constructed microcosms using sterile techniques. In addition to the metal coupon-containing microcosms, reactors without coupons were assembled to assess the effects of YM rock on ground water chemistry.

Table 2. Composition of Alloy 22

C (%*)	Mn (%)	S (%)	Co (%)	Mo (%)	Si (%)	Cr (%)	W (%)	V (%)	Fe (%)	P (%)	Ni (%)
0.002	0.260	0.001	0.510	13.40	0.025	21.58	2.820	0.150	3.95	0.012	Bal.

*weight percent

YM volcanic welded tuff was aseptically collected from the drift walls of the Exploratory Study Facility (ESF,YM, Nevada) in a region adjacent to Alcove 5 which is composed of repository horizon geologic strata (Topopah Springs tuff). Collected tuff was then crushed and sieved (particle size fraction 1-4 mm) using sterile techniques, and stored under sterile conditions, to prevent contamination with microorganisms not associated with post-construction repository conditions. YM Topopah Springs tuff composition[5] is shown in Table 3. To assess the effects of abiotic corrosion, in parallel experiments, aliquots of tuff were sterilized (3-4 Mrad gamma irradiation, as above). Gamma doses of 3 Mrad were sufficient for eradicating the most recalcitrant organisms, while preventing alteration of the tuff composition[6]. Sterility was maintained in these sterilized microcosms by addition of antibiotics (rifampicin, 250 µg/mL; streptomycin, 200µg/mL). Effects of

antibiotics on potential corrosion of material coupons was evaluated by incubating material coupons, in separate control experiments, with 10X J13 media containing antibiotics at these same concentrations. The various microcosm permutations (one of each material type, or no materials), were performed in duplicate.

Table 3. Bulk-rock cation compositions for Topopah Spring tuff at Yucca Mountain, Nevada[5]

	Unaltered lower vitrophyre	Altered lower vitrophyre
Element	**concentration, wt%**	**concentration, wt%**
Si	72.2	69.6
Ti	0.07	0.10
Al	14.3	19.5
Fe^{3+}	0.78	1.07
Mn	0.05	0.06
Mg	0.45	1.33
Ca	0.69	3.73
Na	6.43	3.65
K	4.98	0.91
P	0.01	0.02

Sample Collection, Preparative, and Analytical Techniques

Material Coupons. Alloy 22 coupons were removed from microcosms using sterile techniques, after which a single coupon was immediately fixed in a 2% gluteraldehyde solution for scanning electron microscopy and energy dispersive spectral analysis (SEM/EDS). Following SEM/EDS analyses, a coupon that was microcosm-incubated for one year was washed in 2M HCl for one minute to remove silaceous scale and re-analyzed by SEM/EDS. To gain greater resolution in topological analysis this same coupon was then exposed to Atomic Force Microscopic (AFM) evaluation, and to further evaluate its elemental composition the coupon was characterized with Electron Microprobe/ Wavelength Dispersive Spectroscopy (EM/WDS). The results of these analyses were all compared to those of an Alloy 22 coupon which had not been microcosm-exposed, but which had been subjected to all preparative techniques (i.e., wet polishing, glutaraldehyde fixation, acid washing).

Bulk Solution. Periodically, aliquots of bulk aqueous solution effluxed from microcosm reactors were collected and filtered (0.2 μm) at the reactor outlet. An aliquot was subjected to analysis of pH, then the remaining sample was acidified to pH 2 with HCl to maintain the solubility of contained ions before being analyzed by Inductively Coupled Plasma Atomic Emission Spectrometry (ICP-AES). Transition metals, alkali earth metals, and alkali metals relevant to material coupon composition (Table 2) were quantified.

ICP-AES. Concentrations of those elements relevant to the composition of test coupons (Table 2) were analyzed in bulk aqueous reactor effluents using ICP-AES (Applied Research Laboratories, Model 3560 equipped with a simultaneous optical system, Rowland Circle). Parameters of analysis were: incident power, 1150KW; net gas flow rate, 0.4 L/min; plasma gas flow rate, 16 L/min; reflected power, <2 KW. Concentrations of Co, Cr, Fe, Mn, Mo, Ni, V, and W on samples collected from Alloy 22-containing microcosms were assayed. These elements were also analyzed in solution samples collected from no-metal control microcosms to ascertain the concentration of these elements that are contributed by either the simulated 10XJ13 or solubilized YM rock components.

SEM/EDS. Material coupon surfaces were characterized with a field emission scanning electron microscope (Hitachi S-800) equipped with a Kevex 8000 microanalysis system for image and elemental analyses, respectively. The effective electron beam probe depth was 1 mm. The coupons were coated with carbon to reduce electrical charging of non-conductive materials. Operating parameters for imaging and energy dispersive spectral analysis (EDS) were 16 kV accelerating voltage, 0-10.23 keV range, approximately 1500 cts/sec, and <20% deadtime. The beam was cropped or operated in spot mode during elemental analysis.

AFM Analysis. Atomic Force Microscope (AFM) images were collected with a Digital Instruments Dimension 3100B head operated in the tapping mode.

EM/WDS Analysis. Unreacted and 1-year reacted acid-washed Alloy 22 coupons were analyzed with WDS (JEOL Superprobe 733-LSS). Operating parameters for analysis were as follows: accelerating voltage, 15 kV; and current, 15 nA. Quantitative analysis was performed at magnifications exceeding 120,000X using dQant quantification software. Prior to coupon analysis, elemental standards representative of coupon composition were analyzed for calibration purposes.

RESULTS

Analysis of Aqueous Microcosm Effluents

Aqueous microcosm effluents were monitored over a 427 day period. Aliquots collected for determination of pH indicated that the pH remained in the range of 7-8. ICP-AES analysis revealed that only iron and managanese were detectable among all Alloy 22 components assayed in reactor effluents sampled during this period (Fig. 2). Manganese concentrations rose to approximately 660 ppb in both microcosms containing Alloy 22, as well as in those containing no metal samples. However, the manganese concentrations in Alloy 22-containing reactor effluents required more time to reach the highest concentration observed (Fig. 2). Iron concentrations were lower than those of manganese in both the Alloy 22-containing reactor effluents and no-metal controls, reaching 20-40 ppb iron in both instances (Fig 2).

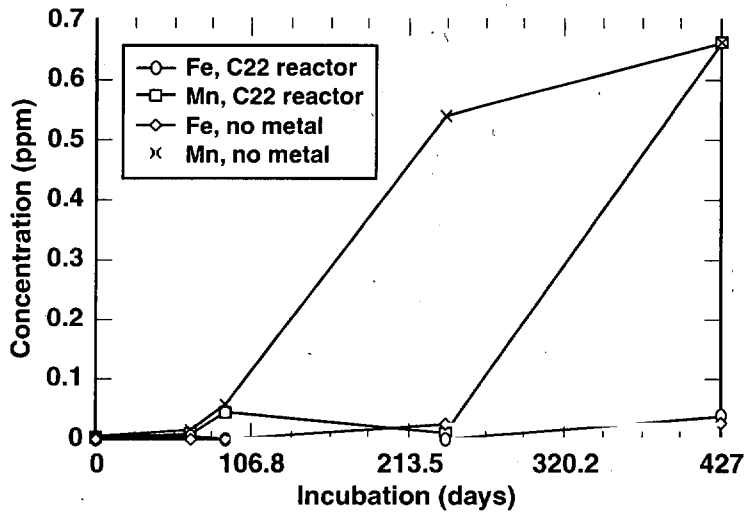

Figure 2. Solubilized Fe and Mn in microcosms containing either Alloy 22 or no-metal controls over a 427 day incubation period. Aqueous metal concentrations were determined by ICP-AES analysis of microcosm effluents. Fe and Mn concentrations in the 10XJ13 media were subtracted from these data (background concentrations of Fe and Mn were 0.005 and 0.0005, respectively). Results are an average of two trials.

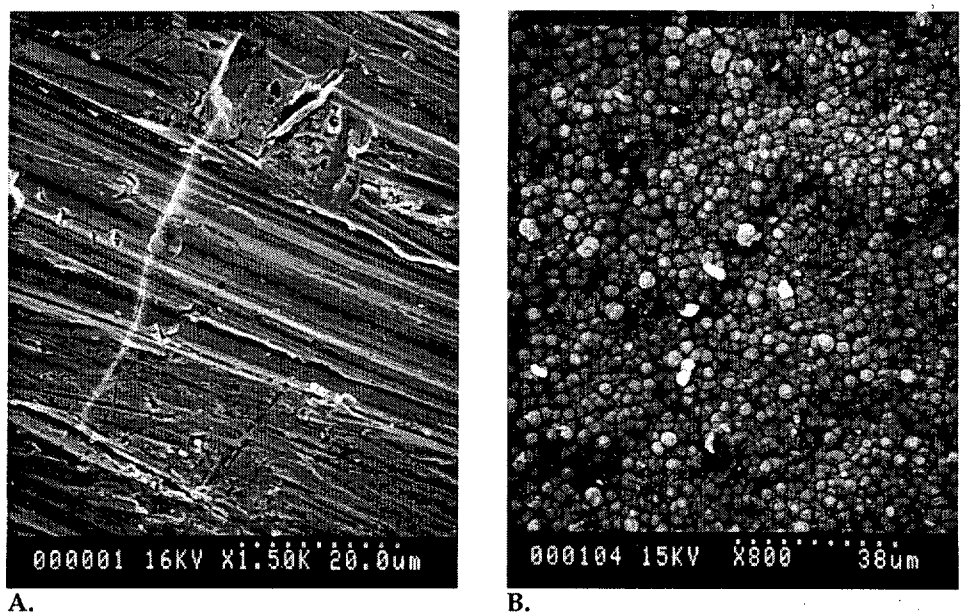

A. B.

Figure 3. SEM photomicrographs of Alloy 22 coupons. Panel A) unreacted coupon surface; Panel B) coating of hemispherical particles composed of Cr and O observed on Alloy 22 after three months microcosm incubation.

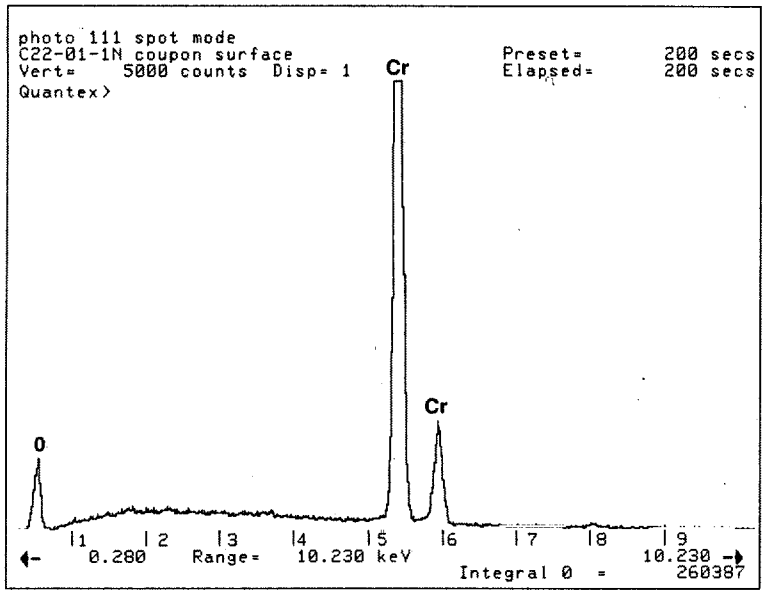

Figure 4. EDS spectrum of a three month microcosm-incubated Alloy 22 surface indicates that the film is composed of Cr and O.

Surfacial Analyses of Microcosm-Exposed Alloy 22 Coupons After Three Months Incubation

Initial SEM image analysis at low magnification (50X) of microcosm-exposed, glutaraldehyde-fixed Alloy 22 after three months exposure in the microcosm environment showed a partially coated coupon surface. The coating was homogeneous and composed of tightly packed hemispherical particles when inspected under higher magnifications (>600X, Fig. 3). EDS analysis of this coating demonstrated that the hemispherical particles were composed of Cr and O; a secondary EDS peak indicating the presence of Mn was not observed showing that Mn was not incorporated into the coating (Fig. 4). In contrast, unexposed/unincubated Alloy 22 showed a polished, uncoated surface without any hemispherical particles, instead demonstrating an array of regular striations resulting from wet polishing (Fig. 3). The portions of the exposed coupon that remained uncoated (appearing at breaks in the coating), was similar in morphology and elemental composition (W, Mo, Ni, Cr, Fe, and V) to unreacted Alloy 22 (Table 3). When a microcosm-exposed, unfixed Alloy 22 coupon was examined, the chromium-enriched coating (previously visualized with SEM/EDS) was not present. Loss of the coating was probably due to its loose adherence to the coupon surface and subsequent spallation; glutaraldehyde

fixation (coupons were fixed on removal from the microcosm, see Methods) was most probably required to detect the presence of the coating. Angular particles scattered on these uncoated coupon surfaces were composed of Al, Si, K, Na, Ca, and O suggestive of a tuff feldspar fines (Na-Ca-K-aluminosilicates); not a precipitated phase, nor originating from corrosion of the alloy.

Surfacial Analyses of Microcosm-Exposed Alloy 22 Coupons After One Year Incubation

Initial observation using SEM of a glutaraldehyde-fixed Alloy 22 coupon after incubation in a microcosm for one year demonstrated an extremely rough surface when compared with unincubated coupons. EDS analysis of this roughened surface showed high levels of silica, indicating the presence of a silaceous scale (data not shown). After coupons were treated with HCl to remove the scale, SEM images (1700X magnification) of microcosm-reacted surfaces still showed that the surface of the microcosm-incubated coupon remained roughened; darkened areas that appeared to be either pits or grain-boundary intrusion were evident even while EDS analysis of these areas showed effective removal of the silica scale (Fig. 5, 6). There were also no other gross differences detected in the EDS spectra for other elements between reacted and unreacted coupons (Fig. 6). While acid-treated unexposed coupons were also roughened due to pre-preparation of all coupons by wet polishing to 600 grit (see Methods), the roughness of the microcosm-incubated coupon was irregular and did not demonstrate the regular array of striations that were evidence of prior wet polishing (Fig. 5).

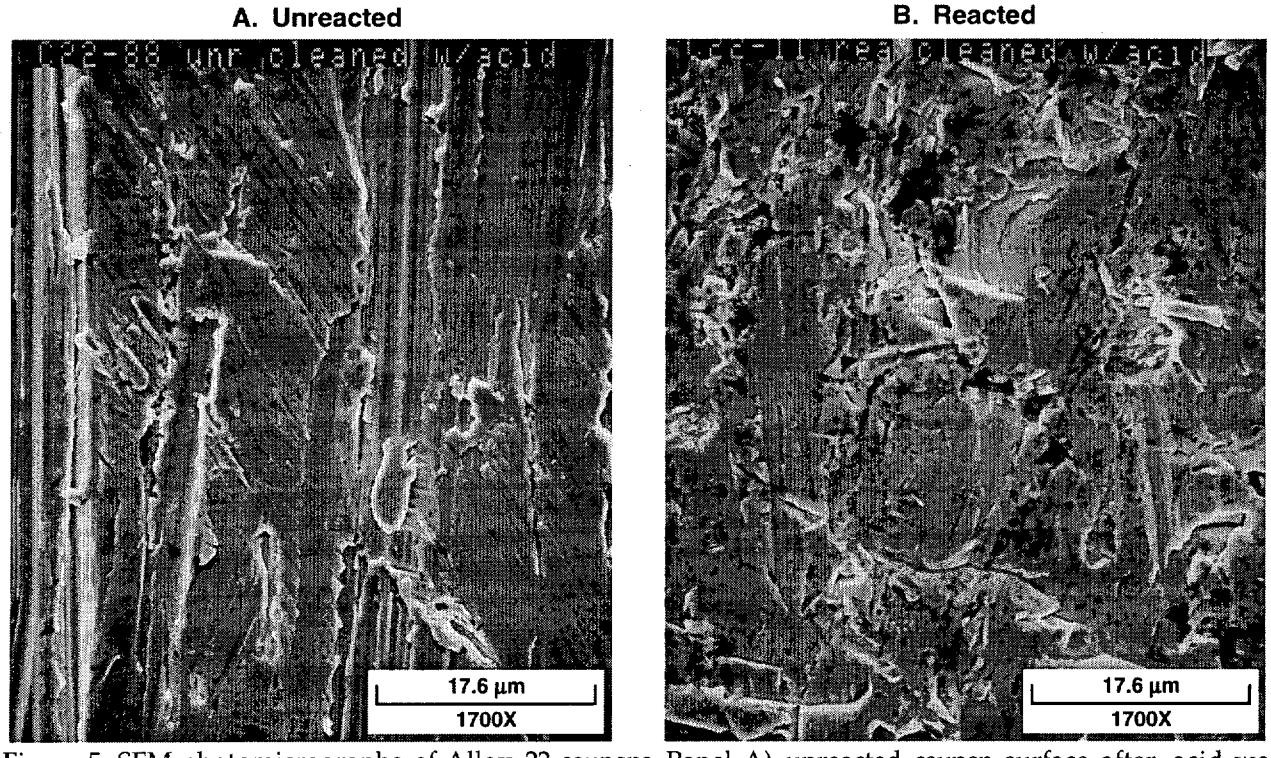

Figure 5. SEM photomicrographs of Alloy 22 coupons. Panel A) unreacted coupon surface after acid-washing; Panel B) coupon surface after one year microcosm incubation followed by acid washing to eliminate scale.

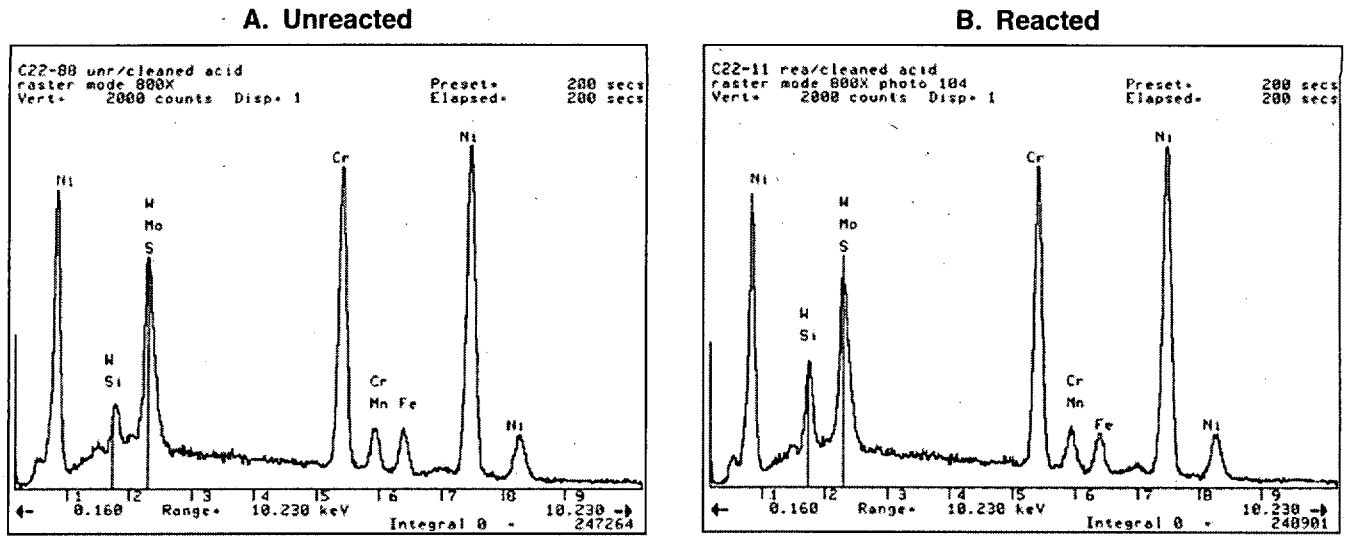

Figure 6. EDS spectra of Alloy 22 coupon surfaces after preparative acid washing to remove scale. Panel A) Alloy 22 unexposed to microcosm; Panel B) Alloy 22 after one year microcosm incubation.

Higher spatial resolution of these surfaces was gained by AFM analysis of acid-washed microcosm-exposed and unexposed coupons. AFM imaging demonstrated regular striations on unincubated, acid-washed coupons of Alloy 22, while pitting was visualized on microcosm-incubated (and acid washed) coupons (Fig. 7). Pits were estimated to be on the order of 1.2μm; however it was not possible to determine the distribution or location of pits on coupon surfaces using this technique. Erosion of the wet polishing striations was evident on microcosm-incubated surfaces, in place of polishing striations both localized and generalized corrosion of these surfaces was observed (Fig. 7).

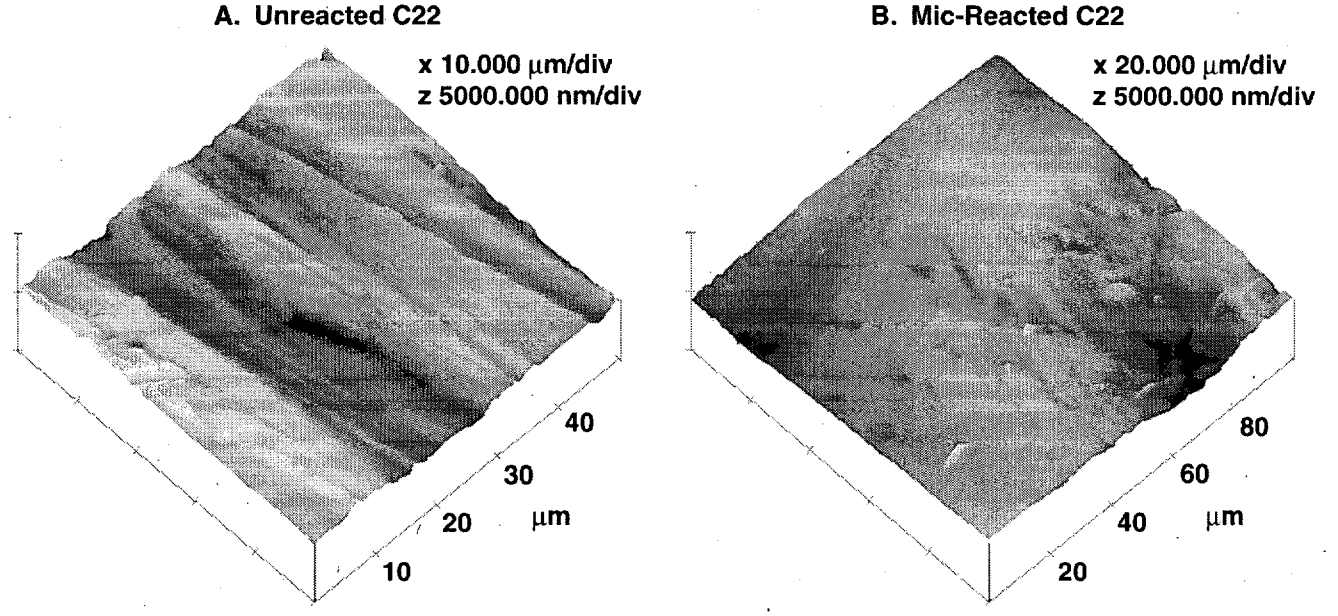

Figure 7. AFM images of Alloy 22 coupon surfaces after preparative acid washing to remove scale. Panel A) Alloy 22 unexposed to microcosms; Panel B) Alloy 22 after one year microcosm incubation.

In an effort to determine whether the imaged pitting on microcosm-exposed Alloy 22 surface was true metal pitting or simply breaks in remnants of the removed silica scale, EM/WDS analyses (which provide greater spatial resolution and quantitative elemental analysis, respectively, compared to SEM/EDS) were performed. Cross sections of the acid-washed, exposed and unexposed coupons were mounted for analyses. Comparison of morphological differences between the two coupons showed that the microcosm-exposed coupon contained more pits than the unexposed coupon. WDS data was collected along transects from one surface of

each coupon towards the opposite surface in order to identify compositional differences within and between the coupons. Transects were also made within the pitted areas and across to the opposite surface to determine preferential metal pitting. The elemental composition of each coupon, after WDS probing, was shown to be identical; the silica content of both coupons was equivalent and representative of the silica concentration in Alloy 22 (data not shown). Further, no siliceous scale was observed in the coupon surfaces

CONCLUSIONS

SEM/EDS analyses of Alloy 22 coupon surfaces incubated in microcosms containing unsterilized YM rock for three months, then glutaraldehyde-fixed, showed a chromium oxide layer composed of hemispherical particles; these were not observed on unexposed and fixed coupon surfaces (Fig. 3). This chromium oxide layer was apparently very loosely adhered to the coupon surface, since when coupons were unfixed and analyzed by other means, or re-analyzed by SEM/EDS, it had been lost by spallation. Despite the presence of this chromium oxide layer, microcosm-incubated coupons showed no immediate gross visible signs of corrosion at the three month sampling point.

Soluble chromium [Cr(VI)] was not detected in bulk solution samples analyzed with ICP-AES. Trivalent Cr [Cr(III), the only other commonly occurring ionic form of Cr] is highly insoluble under oxidizing conditions at circumneutral pH and ambient temperature[7], indicating that the chromium oxide layer is almost certainly a Cr(III) oxide or hydroxide. It is therefore highly plausible that chromium originating from dissolution of the Alloy 22 went into solution as Cr(II), which is highly unstable and spontaneously oxidizes to Cr(III)[7], which then precipitated as a Cr(III) oxide, coating the coupon surface. Dissolution of Cr(0) from metals occurs under certain acidic conditions or upon treatment with reduction processes[7], either of which may have occurred due to bacterial activity in the microcosms. Other investigators have noted that Alloy 22 surfaces become enriched in tungsten and molybdenum under acidified conditions[8], consistent with conditions required for dissolution of Cr(0)[7]. Further, previous studies show dissolution of chromium from Alloy 22 only in the presence of YM bacteria under batch conditions in the presence of a nutrient source [9, 10]. These findings support a loss of chromium during corrosion of Alloy 22 under the microcosm conditions herein described, as evidenced by the accretion of a chromium-containing precipitate. Alternatively, generalized dissolution of Alloy 22 (with only the re-precipitation of chromium onto coupon surfaces) may have occurred with subsequent adsorption of other major Alloy 22 components (nickel, molybdenum) to tuff components; or the formation of nickel silicates. De-alloying of the coupon surface by preferential loss of chromium, or generalized corrosion of Alloy 22, may not have been visible due to the general nature of the corrosion, and occlusion of the coupon surface by the chromium oxide coating.

Aqueous reactor effluents were analyzed for the presence of Alloy 22-containing components over a 14 month period. These results were compared to those from microcosms containing no metal coupons. Comparable low concentrations of iron were found in both the Alloy 22-containing reactors and those containing no metals, indicating that the iron that was observed originated from YM tuff (Fig. 2). Significant and similar final concentrations of manganese were also found in both the control microcosms and those containing Alloy 22, indicating that the detected Mn also originated from tuff. However, there was an additional lag period of over three months in Alloy 22-containing reactors before Mn was detected in reactor effluents (Fig. 2), indicating that perhaps an Alloy 22 component(s) was preventing solubilization of Mn from tuff during this three month period. However, chromium, nickel, or molybdenum-manganese mineral phases all only form under extremely elevated temperatures, thus it appears highly unlikely that any solubilized major Alloy 22 components are mineralizing with dissolved manganese originating from tuff. At this juncture, the delayed detection of solubilized Mn in micocosms containing Alloy 22, which was based on a single sampling point (Fig. 2), remains to be explored.

After a one year incubation different Alloy 22 coupons were withdrawn from microcosms and analyzed. After fixation with glutaraldehyde an extremely roughened surface was evident with SEM analysis. EDS showed that very high levels of silica were contained in the roughened surface indicating the presence of a siliceous scale. While no silica was added to the simulated 10X J13 media feed (Table 1), approximately 70% (weight percent) of YM tuff is composed of SiO_2 (Table 3). Prior similar experiments employing carbon steel coupons demonstrated the precipitation of silica minerals on carbon steel coupons under identical conditions to those employed here[11]. Thus, it is evident that silica solubilizes from tuff and reprecipitates within microcosms. After acid washing, EDS analysis demonstrated that the siliceous scale had been largely

removed, but SEM images still revealed a roughened surface showing evidence of pits, grain boundary attack, or what could be remnants of silica not removed by acid washing, compared with unexposed coupons (Figs. 5, 6). Further analysis employing AFM analysis of microcosm-incubated coupons revealed what appeared to be areas of localized attack, as well as generalized corrosion resulting in the erasure of striations that were created by wet polishing of the coupons (Fig. 7). To determine whether these imaged areas were evidence of true corrosion or simply artifacts from vestiges of unremoved scales EM/WDS analysis was performed and showed that the elemental composition of this area was identical to unexposed coupons, lending support to the supposition that there is some generalized surface degradation of Alloy 22 under conditions that include the presence of YM simulated groundwater, YM rock, and endogenous microorganisms. Solubilized Alloy 22 components may adsorb as ions to tuff mineral surfaces, and nickel can also form silicates under fairly mild conditions. Whether these observed effects are due to the presence of microorganisms must await the analysis of coupons incubated under identical conditions in sterilized systems; these are in progress. Similar experiments are also continuing using coupons of Alloy 22 that have been machined to create a more smooth and uniform surface to better evaluate these putative corrosive effects.

Currently, there is little published information regarding the resistance to MIC of nickel-based alloys using chromium as an alloying element. Two separate studies have shown that Alloy 825 (UNS N08825) was pitted and experienced crevice corrosion in seawater and lakewater when bacteria were present [12,13]. Previous studies conducted in this laboratory employing linear polarization demonstrated a 200-fold increase in the corrosion rate of Alloy 400 (UNS N04400), and a 4-fold increase in the corrosion rate of Alloy 625 (UNS N06625) in the presence of YM bacteria. Subsequent chemical analysis demonstrated a dissolution of nickel from Alloy 400, and dissolution of chromium from Alloy 625[14]. While the current work described here does not unequivocally demonstrate that YM bacteria *per se* are accounting for the observed susceptibility of Alloy 22, these previous reports are consistent with the susceptibility of corrosion resistant Ni-Cr-Mo alloys.

ACKNOWLEDGMENTS

The authors gratefully acknowledge the expert technical services of Anabel Miranda and Terry Duewer in completing this work. This project was conducted under the auspices of the U.S. Department of Energy under contract W-7405-ENG-48, and was supported by the Yucca Mountain Site Characterization Project, LLNL..

REFERENCES

1. T.D. Brock, M.T. Madigan, Biology of Microorganisms, (Englewood Cliffs, NJ: Prentice Hall, 1991): p. 310-311.

2. J.M. Delany, Reaction of Topopah Spring Tuff with Water: A Geochemical Modeling Approach Using the EQ3/6 Reaction Path Code, Lawrence Livermore National Laboratory report, UCID-53631, November, 1985.

3. C.M. Bethke, The Geochemist's Workbench, Version 2.0: A Users Guide to Rxn, Tact, React, and Grplot (Illinois: University of Illinois Hydrogeology Program, 1994).

4. R.D. McCright, "Engineered Materials Characterization Report", vol. 3 rev. 1.1, UCRL-ID-119564, July 1998.

5. . D.E. Broxton, D.L. Bish, R.G. Warren, Clays and Clay Minerals, 35, (1987): pp. 89-110.

6. A .D. McLaren, Radiation as a technique in soil biology and biochemistry, Soil Biol. Biochem. 1, (1969), pp. 63-73.

7. Committee on Biologic Effects of Atmospheric Pollutants, Chromium (Washington D.C.: National Academy of Sciences, 1974), pp.4-6.

8. Joseph Farmer, personal communication.

9. G.G. Geesey, R.J. Gillis, R. Avci, D. Daly, M. Hamilton, P. Shope, G. Harkin, Corrosion Science, 38(1996): p. 73.

10. T. Lian, D. Jones, S. Martin, J. Horn, "A Quantitative Assesment of Microbiological Contributions to Corrosion of Candidate Nuclear Waste Package Materials," Materials Research Society Fall Meeting, (Boston, MA:Material Research Society, 1998); Report UCRL-JC-131555, Lawrence Livermore Natl. Laboratory, October, 1998.

11. J. Horn, S. Masrtin, B. Masterson, and T. Lian, "Biochemical contriutions to corrosion of carbon steel and alloy 22 in a continual flow system," CORROSION/99, paper no. 162 , (Houston, TX:NACE Intl., 1999).

12. A.M. Brennenstuhl, P.E. Doherty, P.J. King, and T.G. Dunstall, The effects of biofouling on the corrosion of nickel heat exchanger alloys at Ontario Hydro, *in* Microbially Influenced Corrosion and Biodeterioration. N.J. Dowling, M.W. Mittelman, and J.C. Danko, eds. (Knoxville, TN:The University of Tennessee, 1990), pp 4-25 to 4-31.

13. S.C. Dexter, K.E. Lucas, and G.Y. Gao, The role of marine bacteria in crevice corosion initiation, *in* Biologically Induced Corrosion, S.C. Dexter, ed. (Houston, TX: National Assoc. of Corrosion Engineers), pp. 144-153.

14. T. Lian, S., Martin, D. Jones, A. Rivera, and J. Horn, "Corrosion of candidate container materials by Yucca Mountain bacteria", CORROSION/99, paper no. 476, (Houston, TX:NACE Intl., 1999); Report UCRL-JC-132825, Lawrence Livermore Natl. Laboratory, January, 1999.